J. Condensed Matter Nucl. Sci. 8 (2012) 124–131

Research Article

# Nuclear Signatures to be Expected from Rossi Energy Amplifier*

Jacques Dufour †

*CNAM Laboratoire des sciences nucléaires, 2 rue Conté 75003 Paris, France*

**Abstract**

The nuclear signatures that can be expected when contacting hydrogen with fine nickel powders are derived from thermal results recently obtained (Rossi energy amplifier). The initiation of the reactions (either by proton or neutron capture) is not discussed and considered as true. Proposals are made to check the process either by radiation emission measurements or by elemental analysis (ICP-MS)
 ISSN 2227-3123

*Keywords:* Energy production, Hydrogen, Nickel, Nuclear reaction, Radiations

## 1. Introduction:

In a recent paper [1], results are presented on vast amounts of energy (kWh) generated by contacting Hydrogen at pressures of tens of bars and temperatures round 400°C, with nickel powder (with an unspecified additive). No harmful radiations were measured, which is attributed to the presence of a lead shield absorbing $\gamma$ emission occurring during the run and to the very short period of the instable species formed during the run and decaying after shut down. The efficiency of the process is very high ($E_{out}/E_{in}$ up to 400). These levels of energy production strongly points to a nuclear origin. The proposed process [1] would be proton capture by the nickel nuclei.

The coulomb barrier problem is suggested to be solved by the strong screening of the electrons. Another solution has been proposed [2]: virtual neutrons formation, reacting with the Nickel nuclei. This solution is also proposed in [3] with a very elaborate justification.

In this paper, the capture of a neutron or a proton by a nickel nucleus is accepted as real. The consequences of these captures are analyzed (using very well documented nuclear chemistry data [4,5] and proposals are made for precise verification of the process invoked.

*A first version of this paper has been published in *J. Nucl. Phys.* on 6 May 2010. This improved version may slightly differ from the first one.

†E-mail: 3jdufour@laposte.net

 ISSN 2227-3123

**Table 1.** Neutron capture

| Ni parent isotopic composition | Ni parent nucleus | Mass parent or daughter Ni nucleus | Energy (MeV) released | Excited intermediate nucleus | Decay intermediate nucleus ground state | End s table nucleus | Natural copper isotopic composition |
|---|---|---|---|---|---|---|---|
| 0.68007 | $^{58}$Ni | 57.935346 | 8.22 | $^{59}$Co | EC, 7.5 $10^4$y, 1.07 | $^{59}$Co | |
| | $^{59}$Ni | 58.934349 | | | | | |
| 0.26223 | $^{60}$Ni | 59.930788 | 7.04 | $^{61}$Ni* | | $^{61}$Ni | |
| 0.0114 | $^{61}$Ni | 60.931058 | 9.82 | $^{62}$Ni* | | $^{62}$Ni | |
| 0.03634 | $^{62}$Ni | 61.928346 | 6.06 | $^{63}$Ni* | $\beta^-$,100 y,0.066 | $^{63}$Cu | 0.6917 |
| | $^{63}$Ni | 62.929669 | | | | | |
| 0.00926 | $^{64}$Ni | 63.927968 | 5.32 | $^{65}$Ni* | $\beta^-$,2.52 h,2.14 | $^{65}$Cu | 0.3083 |
| | $^{65}$Ni | 64.930086 | | | | | |

## 2. The Neutron or Proton Capture by Nickel :

The reactions paths for these 2 routes finally ends up to the same stable products ($^{59}$Co, $^{61}$Ni, $^{62}$Ni, $^{63}$Cu and $^{65}$Cu) and are summarized in Tables 1 and 2.

The energy release (see Table 3) occurs mostly by de-excitation through $\gamma$ emission of the intermediate excited Ni* compound nucleus. The characteristics of this $\gamma$ emission (depending upon the levels of the excited nucleus). are very well known [4]. This represents (on average) some 8 MeV (balance after deduction of the energy required for the "virtual neutron" formation, i.e 0,782 MeV). The remaining comes from the decay of the ground states of the radioactive intermediate species formed ($^{59}$Ni, $^{63}$Ni and $^{65}$Ni). Data for intermediate radioactive species are from [5]. In the column "Decay intermediate nucleus ground state" 3$^{rd}$ figure is the energy of the emitted radiation (MeV).

The energy is released in a way very similar to the neutron capture route, with a lower release from the de-excitation of the intermediate excited Cu* compounds nucleus (some 4 MeV, see Table 3). The remaining half comes from the decay of the ground states of the radioactive intermediate species formed ($^{59}$Cu, $^{59}$Ni, $^{61}$Cu and $^{62}$Cu). Data for intermediate radioactive species are from [5].

**Table 2.** Proton capture

| Ni parent isotopic composition | Ni parent nucleus | Mass of parent Ni nucleus | Mass of daughter Cu nucleus | Energy (MeV) released | Excited intermediate nucleus | Decay intermediate nucleus ground state | End s table nucleus | Natural copper isotopic composition |
|---|---|---|---|---|---|---|---|---|
| 0.68007 | $^{58}$Ni | 57.935346 | | $^{59}$Cu* | $\beta^+$, 82$s$, 4.8 | $^{59}$Ni=$^{59}$Co | See note | |
| | $^{59}$Ni | | 58.939503 | | | | | |
| 0.26223 | $^{58}$Ni | 59.930788 | | 4.8 | $^{59}$Cu* | $\beta$*, 82s, 4.8 | $^{59}$Ni= $^{59}$Co | See note |
| 0.0114 | $^{60}$Ni | | 4.8 | $^{61}$Cu* | $\beta$, 3.41 h, 2.34 | $^{61}$Ni | | |
| | 59.930788 | | | | | | | |
| 0.03634 | $^{62}$Ni | 6.928346 | 61.932586 | 6.12 | $^{63}$Cu | | $^{63}$Cu | 0.6917 |
| | $^{63}$Ni | | 62.929598 | | | | | |
| 0.00926 | $^{64}$Ni | 63.927968 | | 7.45 | $^{65}$Cu | | $^{65}$Cu | 0.3083 |
| | $^{65}$Ni | | 64.927793 | | | | | |

*Note*: $^{59}$Ni from $^{59}$Cu decays to $^{59}$Co by electron capture (life time $7.5 \times 10^4$ years).

**Table 3.** Energy released (MeV)

| | Neutron capture | Proton capture |
|---|---|---|
| De-excitation | 7.82 | 3.94 |
| Decay | 0.02 | 3.92 |
| Total | 7.84 | 7.86 |

## 3. Evaluation of the Reaction Rates

One experiment (Type B) presented in [1] has yielded 3768 kWh for an energy input of 18.54 kWh (between March 5, 2009 and April 26, 2009). This is a net power produced of some 3 kW during a time $T$ of some $4.5\times10^6$ s. The rate of production of the by-products will be determined using this net produced power, according to the proton and the neutron reaction scheme. The time $T$ will be used to calculate the amount of reaction products present at the end of the experiment.

From Tables 1 and 2, the energy released per Ni atom (averaged by the isotopic composition of the Nickel) has been calculated under following hypothesis:

(1) The captures (proton or neutron) have the same probabilities whatever the Ni isotope is. This is a first approximation. For the neutron capture route, following cross sections (barn) are measured: $^{58}$Ni:4.6, $^{60}$Ni:2.9, $^{61}$Ni:2.5, $^{62}$Ni:15 and $^{64}$Ni:2.9).
(2) The subsequent reactions with formed products are not taken into account (too low concentration to have a ny significant effect).
(3) Decay energy of nucleus with half life time much longer than the experiment duration have been ignored ($^{59}$Ni for the proton route and $^{59}$Ni, $^{63}$Ni for the neutron route).

Table 3 is thus obtained.

As expected, the two routes give similar amounts of energy, mainly de-excitation for the neutron route and half de-excitation, half decay for the proton route.

The proton or neutron capture rate can thus be evaluated as

$$r = \frac{3000}{7.85\times1.6\times10^{-13}} = 2.4\times10^{15}\ \mathrm{s}^{-1}$$

for both routes

## 4. Evaluation of the $\gamma$ Emission Rates

The de-excitation of a compound nucleus resulting from neutron capture is very well documented [4]. For nickel, one capture gives rise to 2.66 emission of $\gamma$ photon, with an energy repartition $f_i$ given in Table 4.

For the proton capture route, less data are available. To get a first order of magnitude of the $\gamma$ emission coming from the de-excitation of the primary nucleus formed, the same number of photons per proton capture with the same energy repartition as for the nickel has been taken into account, with of course an average value half the one for nickel (1.79 MeV compared to 3.58). The second half of the energy comes (in the form of $\gamma$ photons) from the short live $\beta+$ emitters: associated $\gamma$ emission, bremsstrahlung of the positron and annihilation radiation. The average energy of these photons is taken to be in the 0.75 MeV range, thus less penetrating. The energy repartitions $f_i'$ (Table 5) have been evaluated according to the photon production rate in the proton capture route given below.

**Table 4.** Neutron capture

| $\gamma$-Energy (MeV) | Repartition ($f_i$) | Absorption coefficient, $\mu$ ($cm^{-1}$) |
|---|---|---|
| 0.5 | 0.32 | 0.578 |
| 1.5 | 0.15 | 0.045 |
| 2.5 | 0.09 | 0.0229 |
| 4 | 0.09 | 0.024 |
| 6 | 0.13 | 0.0398 |
| 8 | 0.22 | 0.079 |
| Mean value | 3.58 | 1.0 |

Finally, the $\gamma$ photon production rate $r_\gamma$ for both routes has been evaluated as follows:

(a) Neutron capture route $(r_\gamma)_{\mathrm{N}} = 2.66r$

(b) Proton capture route $(r_\gamma)_{\mathrm{p}} = 2.66r\left(0.5 + \frac{0.5\times(E_\gamma)_{\beta+}}{2.66\times 0.75}\right) = 2.66r(0.5 + 0.9825)$

$(E_\gamma)_{\beta+}$ being the mean energy released by $\beta+$ emissions (3.92 MeV).

## 5. Effect of Lead Shielding on Expected $\gamma$ Emission

For a poly-energetic beam of photons, the attenuation $l/l_0$, resulting from a thickness $d$ of lead, is

$$l/l_0 = \sum_i f_i \exp(-d\mu_i)$$

is the fraction of the beam of energy $E_i$ and $\mu_i$ $f_i$ the absorption coefficient for photons of energy $E_i\,(\mathrm{cm}^{-1})$ and $d$ (cm).

In [6], the quantity $\mu/\rho$ ($\mathrm{cm}^2/\mathrm{g}$) is given for photon energies from 1 eV to 20 MeV. This gives for lead ($\rho = 11.34\,\mathrm{g/cm}^{-3}$), the absorptions coefficients $\mu_i$ (Tables 4 and 5).

Finally, following relations were used to evaluate the attenuation of the beam for increasing values of

**Table 5.** Proton capture

| $\gamma$-Energy (MeV) | Repartition ($f_i'$) | Absorption coefficient, $\mu$ ($cm^{-1}$) |
|---|---|---|
| 0.25 | 0.18 | 1.136 |
| 0.75 | 0.51 | 0.139 |
| 1.25 | 0.05 | 0.058 |
| 2 | 0.05 | 0.045 |
| 3 | 0.07 | 0.061 |
| 4 | 0.14 | 1.111 |
| Mean value | 1.79 | 1.0 |

$d$ ($f_i$ from Table 5)

$$\text{Neutron capture route} \qquad \frac{l}{l_0} = \sum_i f_i \exp(-\mu_i d),$$

$$\text{Proton capture route} \qquad \frac{l}{l_0} = \sum_i f_i \exp(-\mu_i d).$$

As expected, the lead shielding is more efficient in the proton capture route. Even in that case and for 40 cm of lead, the transmitted activity is still $10^6\ s^{-1}$. The corresponding value is $3\times10^{10}\ s^{-1}$ in the neutron capture route.

An important point must be stressed: in the above calculation, the emitting nuclear source is considered to be concentrated in one single point, which is of course not the case. To get a realistic evaluation of the expected flux of photons, it is supposed that the Nickel powder is contained in a cylindrical reactor, diameter 2 cm and length 100 cm (outer surface 628 $cm^2$). At 1 m from this tube, shielded by 40 cm of lead, the photons flux (number of particles emitted in the solid angle under which the source is seen from the point where the flux is evaluated), is thus $\approx 1\ s^{-1}cm^{-2}$ for proton capture and $\approx 5\times10^3\ s^{-1}cm^{-2}$ for neutron capture.

## 6. Final Products and Residual Activity after Shut Down

The number of stable atoms $i$ formed at the end of the experiment (time $T$) is

$$N_i(T) = r_i T = r x_i T.$$

For radioactive atoms with a disintegration constant $\lambda_i$, the number of atoms formed at $T$ is

$$N_i(T) = \frac{r x_i}{\lambda_i}(1 - e^{-\lambda_i T})$$

For short life atoms ($^{59,61\text{ and }62}$Cu-proton capture- $^{65}$Ni-neutron capture-), the asymptotic limit is reached well before $T$ and the number of atoms at $T$ is

$$N_i(T) = \frac{r x_i}{\lambda_i}.$$

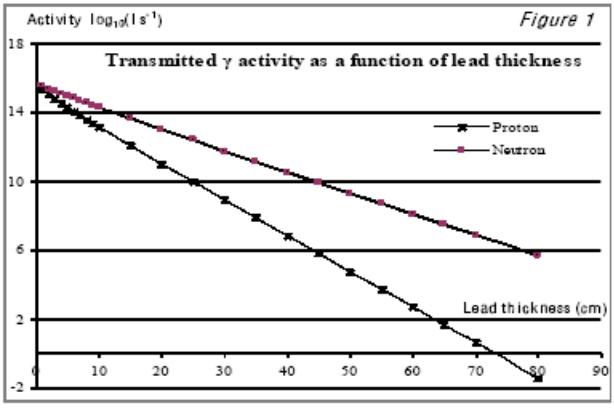


**Figure 1.** Gives the transmitted $\gamma$ activity (as $\log_1 0(I.s^{-1})$, as a function of the lead thickness $d$.

For long life atoms ($^{59\text{ and }63}$Ni-neutron capture and $^{59}$Ni-proton capture), the final product at T can be considered to be $^{59\text{ and }63}$Ni on the one hand and $^{59}$Ni on the other.

Tables 6 and 7 summarize the various atoms formed at the experiment shut-down.

The figures indicated in the last column of Tables 6 and 7 are for an energy production of 3 kW during time $T$ (see Section 3).

## 7. Residual Activity after Shut Down

For both routes, short live species are formed: $^{65}$Ni for neutron capture and $^{59,61}$ and $^{62}$Cu for proton capture (see Tables 1,2,6 and 7). Their concentrations at shut down Ni($T$) are given in Tables 6 and 7. The number of short live species decreases as $N_i(t) = N_i(T)\mathrm{e}^{\lambda_i t}$ ($t = 0$ at shutdown) and their residual activity decreases exponentially with time $t$ after shut down as

$$\frac{\mathrm{d}N_i(t)}{\mathrm{d}t} = -\lambda_i N_i(T)\mathrm{e}^{\lambda_i t}(\mathrm{s}^{-1}).$$

Table 8 gives Ni($T$) at shutdown (after duration $T$ of the experiment) and the remaining atoms at $t = 7200$ s (2 h after shut down) $_{N(7200)} = N_i(T)\mathrm{e}^{-7200O\lambda_i}$ and hence the zero residual activity at that time

$$\frac{\mathrm{d}N_i(7200)}{\mathrm{d}t} = -\lambda_i N_i(7200)(\mathrm{s}^{-1}).$$

The numerical value is given for $t = 7200$ s, this value providing sufficient time to dismantle the experiment after shut-down.

Tables 8 and 9 give the residual activity 2 hours after shutdown. The energy of the main characteristic gammas are given in keV and the branching ratios in % (between brackets).

It can be seen from Table 8 (neutron capture), that 2 h after shutdown, the activity of $^{65}$Ni is still $1.3 \times 10^{13}\mathrm{s}^{-1}$. For proton capture (Table 9) the corresponding activity of $^{61}$Cu is still $4.2 \times 10^{14}\mathrm{s}^{-1}$.

As for the emission during the run, the emitting nuclear source is considered to be concentrated in one single point, which is of course not the case. If, as supposed previously, the Nickel powder is contained in a cylindrical reactor, diameter 2 cm and length 100 cm, the total weight of nickel is some 1260 g (apparent density 4, volume 300 $\mathrm{cm}^3$). If 3 $\mathrm{cm}^3$ of the powder is placed against a germanium detector, the activity would be reduced to some $10^{11}/10^{12}\mathrm{s}^{-1}$ and characteristic radiations could be measured (annihilation radiation for $^{61}$Cu and characteristic gammas (see Table 8) for $^{65}$Ni). Note that if the actual mass of nickel used is m, all results indicated in Tables 6–9 are to be multiplied by m/1260)

**Table 6.** Neutron capture

| Ni parent composition ($X_i$) | Intermediate ground state nucleus | Disintegration constant $\lambda(\mathrm{s}^{-1})$ | Intermediate ground state atoms at $T$ | First (or final) daughter nucleus | Stable atoms formed at $T$ ($^{59}$Ni and $^{63}$Ni are "quasi-stable": they decay slowly to $^{59}$Co and $^{63}$Cu) | |
|---|---|---|---|---|---|---|
| 0.68007 | $^{59}$Ni | $2.90\times10^{-13}$ | $7.32 \times 10^{21}$ | $^{59}$Co | $^{59}$Ni | $7.32 \times 10^{21}$ |
| 0.26223 | $^{61}$Ni | | | | $^{61}$Ni | $2.82 \times 10^{21}$ |
| 0.0114 | $^{62}$Ni | | | | $^{62}$Ni | $1.23 \times 10^{20}$ |
| 0.03634 | $^{63}$Ni | $2.20\times10^{-11}$ | $3.91 \times 10^{20}$ | $^{63}$Cu | $^{63}$Ni | $3.91 \times 10^{20}$ |
| 0.00926 | $^{65}$Ni | $7.64 \times 10^{-5}$ | $2.90 \times 10^{17}$ | $^{65}$Cu | $^{65}$Cu | $9.97 \times 10^{19}$ |

**Table 7.** Neutron capture

| Ni parent composition ($X_i$) | Intermediate ground state nucleus | Disintegration constant $\lambda(s^{-1})$ | Intermediate ground state atoms at $T$ | First (or final) daughter nucleus | Stable atoms formed at $T$ ($^{59}$Ni and $^{63}$Ni are "quasi-stable": they decay slowly to $^{59}$Co | |
|---|---|---|---|---|---|---|
| 0.68007 | $^{59}$Cu | $8.45 \times 10^{-3}$ | $1.93 \times 10^{17}$ | $^{59}$Ni | $^{59}_{Ni}$ | $7.30 \times 10^{21}$ |
| 0.26223 | $^{61}$Cu | $5.65 \times 10^{-5}$ | $1.11 \times 10^{19}$ | $^{61}$Ni | $^{61}$Ni | $2.82 \times 10^{21}$ |
| 0.0114 | $^{62}$Cu | $1.19 \times 10^{-3}$ | $2.3 \times 10^{16}$ | | $^{62}$Ni | $1.22 \times 10^{20}$ |
| 0.03634 | $^{63}$Cu | | | | $^{63}$Cu | $3.90 \times 10^{20}$ |
| 0.00926 | $^{65}$Cu | | | | $^{65}$Cu | $9.94 \times 10^{19}$ |

## 8. Transmuted Products Formed

If the total amount of nickel supposed to be processed is some 1260 g, corresponding to 21.7 mol or $1.30 \times 10^{25}$ atoms, a tentative mass balance can be made.

For both routes, the isotopic composition of the Nickel is not significantly altered. For both routes, a sizeable amount of "quasi-stable" $^{59}$Ni is produced, that represent more than 500 ppm atoms of the starting nickel. This is far beyond the precision of Mass spectrometry and could thus be easily detected. In the neutron capture route, "quasi-stable" $^{63}$Ni could also be detected (50 ppm atoms).

As regards the isotopic ratio of copper $^{63}\text{Cu}/^{65}\text{Cu} = 2.244$, it should increase in the proton capture route (the copper produced has a ratio of 3.92). It should decrease in the neutron capture route (no $^{63}$Cu is produced). The copper produced represents some 7 ppm atoms in the neutron route and some 37 ppm atom in the proton route. Starting from Nickel powder containing around 1 ppm Copper should give reliable indications of the process.

## 9. Conclusion

Strong nuclear signatures are expected from the Rossi energy amplifier and it is hoped that this paper can help detect them.

It is of interest to note that in [3] a mechanism is proposed, that strongly suppresses the gamma emission during the run (it is the same mechanism that creates very low energy neutrons, subsequently captured by the nickel. This does not suppress the emission after shut-down, which should be observed, together with the transmutations described above.

**Table 8.** Neutron capture

| Ni parent composition ($X_i$) | Intermediate ground state nucleus | Disintegration constant $\lambda(s^{-1})$ | Ni($T$)(atoms) | Ni(7200)(atoms) | Acivity after 2 h $dNi/dt$ ($s^{-1}$) | Main gamma photons (keV) (%) |
|---|---|---|---|---|---|---|
| 0.68007 | $^{59}$Cu | $8.45 \times 10^{-3}$ | $1.93 \times 10^{17}$ | $7.13 \times 10^{-10}$ | $6.03 \times 10^{-12}$ | 511, (196) |
| 0.26223 | $^{61}$Cu | $5.65 \times 10^{-5}$ | $1.11 \times 10^{19}$ | $7.41 \times 10^{18}$ | $4.19 \times 10^{14}$ | 511, (122) |
| 0.0114 | $^{62}$Cu | $1.19 \times 10^{-3}$ | $2.3 \times 10^{16}$ | $4.46 \times 10^{12}$ | $5.3 \times 10^{9}$ | 511, (196) |
| 0.03634 | $^{63}$Cu | | | | | |
| 0.00926 | $^{65}$Cu | | | | | |

**Table 9.** Proton capture

| Ni parent composition ($X_i$) | Intermediate ground state nucleus | Disintegration constant $\lambda(s^{-1})$ | Ni($T$)(atoms) | Ni(7200)(atoms) | Acivity after 2 h $dNi/dt$ ($s^{-1}$) | Main gamma photons (keV) (%) |
|---|---|---|---|---|---|---|
| 0.68007 | $^{59}$Cu | $8.45 \times 10^{-3}$ | $1.93 \times 10^{17}$ | $7.13 \times 10^{-10}$ | $6.03 \times 10^{-12}$ | 511, (196) |
| 0.26223 | $^{61}$Cu | $5.65 \times 10^{-5}$ | $1.11 \times 10^{19}$ | $7.41 \times 10^{18}$ | $4.19 \times 10^{14}$ | 511, (122) |
| 0.0114 | $^{62}$Cu | $1.19 \times 10^{-3}$ | $2.3 \times 10^{16}$ | $4.46 \times 10^{12}$ | $5.3 \times 10^{9}$ | 511, (196) |
| 0.03634 | $^{63}$Cu | | | | | |
| 0.00926 | $^{65}$Cu | | | | | |

## References


[1] S. Focardi and A. Rossi, A new energy source from nuclear fusion, *J. Nucl. Phys.*, http://www.journal-of-nuclear-physics.com, February 28 2010

[2] L. Daddi, Virtual neutrons in orbital capture and neutron synthesis, *J.Nucl. Phys.* http://www.journal-of-nuclear-physics.com, March 18 2010

[3] Widom Larsen, Theoretical Standard Model rates of proton to neutron conversions near metallic hydride surfaces, *New Energy time Widom-Larsen portal*.

[4] A. Bauer, Protection contre les rayonnements, Commissariat à l'énergie atomique ISBN 2-7272-0102-8.

[5] IAEA. ENSDF. Nuclear data service, 2009. `http://www-nds.iaea.org/`.

[6] -NISTX-Ray-Mass-attenuation-Coefficients-Lead
`http://physics.nist.gov/PhysRefData/XrayMassCoef/ElemTab/z82.html`